

Research

## Enhancing mechanical performance of biodegradable automotive composites with EPO and graphene

N. Jiyas<sup>1,3</sup> · Indu Sasidharan<sup>2,3</sup> · K. Bindu Kumar<sup>1,3</sup>

Received: 3 October 2023 / Accepted: 17 January 2024

Published online: 22 January 2024

© The Author(s) 2024 [OPEN](#)

### Abstract

Recent strides in composite manufacturing technology have sparked a widespread embrace of natural fiber composites in engineering applications, exemplified by flax fiber. The crux of this development centers on the creation of an environmentally friendly composite, utilizing alkali-treated flax fiber reinforcement and poly lactic acid (PLA) as the polymer matrix through a hot compression technique. The investigation into water absorption unveils that alkaline treatment augments the hydrophobic nature and enhances the crystallinity of flax fibers, resulting in improved adhesion between the reinforcement and polymer matrix. The introduction of 5% wt of epoxidized palm oil (EPO) as plasticizers not only counters brittleness but also elevates thermal stability. Further enhancements are achieved through the addition of 0.5 wt% of graphene nanoparticles as nano-fillers, culminating in superior mechanical properties. This research places a focal point on a thorough mechanical characterization of these green composites, encompassing tensile, flexural, and impact properties, along with an assessment of inter-laminar shear strength. A detailed analysis of dimensional stability is conducted, while morphological scrutiny is performed using scanning electron microscopy. This study marks a significant leap towards sustainable engineering, presenting innovative natural fiber green composites that exhibit heightened mechanical and environmental performance.

**Keywords** Bio-degradable composite · Epoxidized palm oil · Flax fiber · Graphene nanopowder · Natural fibers · Poly lactic acid

## 1 Introduction

Recent years have witnessed significant progress in composite manufacturing technology, especially concerning the adoption of polymer matrix composites in diverse engineering applications [1, 2]. One noteworthy application involves the utilization of graphene and Mn-Zn ferrite polylactic acid (PLA) composites. These composites are fabricated using fused deposition molding with composite wires in 3D printing, resulting in materials with impressive microwave absorption capabilities and load-bearing capacity [3]. Another application is the use of green composites in automobiles formulated from soy protein, PLA [4]. These natural fiber composites are preferred due to their adaptability, cost-efficiency, and straightforward manufacturing processes. The literature has extensively explored the use of natural fibers as reinforcing elements in composites alongside epoxy resin. These discussions have covered the distinctive characteristics of each natural fiber and the potential applications and capabilities of these composite materials [5]. However, their

---

✉ K. Bindu Kumar, [2bindukumar@gmail.com](mailto:2bindukumar@gmail.com) | <sup>1</sup>Department of Mechanical Engineering, Government Engineering College, Thiruvananthapuram, Kerala, India. <sup>2</sup>Department of Chemistry, Government Engineering College, Thiruvananthapuram, Kerala, India. <sup>3</sup>APJ Abdul Kalam Technological University, Thiruvananthapuram, Kerala, India.



non-biodegradable nature with epoxy resin is a significant drawback in the context of environmental sustainability. In response, the scientific community has been exploring the development of "green composites," which are more environmentally friendly. Green composites are created by reinforcing biopolymers with natural fibers such as coir, flax, sisal, bamboo, and more [6]. Biopolymers like starch and Polypropylene (PP), Polystyrene (PS), Polyethylene (PE), and PLA are commonly used for making these green composites [7]. Some combinations involve partially or fully biodegradable natural fibers like jute and sisal combined with synthetic polymers like polypropylene (PP) or natural materials like polylactic acid (PLA). When incorporating Rice Residue into PLA composites, there is a noteworthy enhancement in mechanical, thermal, and degradation properties. Notably, as the rice residue content increases, the biodegradability of these composites also exhibits a corresponding increase [8]. Recent research has also highlighted the inconsistent behavior of natural fibers in fiber metal laminates. Notably, in mechanical tests, it was observed that these laminates exhibited superior performance when the jute layers were placed between the basalt fibers, whereas their mechanical properties significantly declined when the basalt fibers were sandwiched between the jute layers [9]. However, when a small amount (0.3 wt%) of carbon nanotubes (CNTs) was introduced, these fiber metal laminates demonstrated notable enhancements in flexural strength, flexural modulus, and shear strength [10]. Notably, PLA composites tend to have higher tensile and flexural moduli than their PP counterparts [11]. The choice of biopolymers is driven by factors such as cost, dimensional stability, and hardness [12]. PLA, for instance, is a popular choice due to its affordability, stability, and rigidity, but low melting point [13]. Numerous studies have explored hybrid combinations of natural fibers [14], and experiments with abaca-reinforced polypropylene composites have demonstrated better resistance to crack formation [15]. However, one common challenge in green composites is the need for proper adhesion between the fibers and the matrix, which can lead to the degradation of mechanical properties. Natural fibers are also inherently hydrophilic due to the presence of hydroxyl groups, making them susceptible to moisture-related issues [16].

To address these challenges, various treatments are applied, including chemical (e.g., silane, acetone, and alkali treatment), physical, and biological methods [17]. Among these, alkali treatment using sodium hydroxide (NaOH) or potassium hydroxide (KOH) is preferred. This treatment modifies the fiber's structure and surface, improving adhesion. Flax fibers, chosen as reinforcement material in this work, are treated with a 2% NaOH solution at room temperature for 2 h [18, 19]. This process not only enhances mechanical properties but also removes surface impurities [20, 21].

Plasticizers are introduced into green composites to combat PLA's brittleness and low impact resistance, which serves as the resin [22]. For example, epoxidized soybean oil methyl ester (ESOME) is a plasticizer that biodegrades fast when blended with PLA, improving brittleness in industrial composting settings [23]. Epoxidized palm oil (EPO), an epoxidized derivative of glycerol esters with various fatty acids, enhances thermal stability and flexibility in PLA/EPO blended composites [24, 25]. The addition of nano-fillers, like graphene nanoparticles, has been found to significantly improve mechanical properties [26, 27]. For instance, 1% graphene nanoparticles in a PLA/EPO blend can increase tensile strength by 26% and impact strength by 73% [28].

The primary objective of this study is to perform a comprehensive mechanical characterization of a green composite (FLAX/PLA) (laminated 1) made from natural fibers, specifically flax fibers, and utilizing PLA as the polymer matrix. To overcome the effect of hydroxyl group in the flax fibers, the fibers were alkaline treated with NaOH solution. Water absorption tests were carried out before and after the alkaline treatment to ensure that the effect of hydroxyl group is minimized. The composites were modified with EPO addition (FLAX/PLA/EPO) (laminated 2) and later again modified with addition of graphene (FLAX/PLA/EPO/GN) (laminated 3) as a nano filler. The weight percentage of EPO [24, 25] and graphene [27, 29] were selected from literature. Tensile, flexural, impact tests and inter laminar shear strength of all the three laminates were analyzed. Morphological analysis of the laminates was carried out using scanning electron microscopy. Physical characterization of the prepared laminates was studied in depth. The development of this novel natural fiber green composite marks a significant stride in the direction of sustainable engineering.

## 2 Materials and methods

### 2.1 Raw materials

Poly(lactic acid) (PLA) (Grade-3052D) used for matrix was purchased from Nature Tec India Pvt. Ltd Chennai, Tamil Nadu, India. The PLA had density of 1.24 g/cm<sup>3</sup> and melting point 190 °C, as per supplier specification. The flax fiber in the form of balanced bidirectional woven fabric 0°/90° with 350 gsm was supplied by DLS Traders, Salem, Tamil Nadu, India. So obtained flax fibers were chemically treated as reported [30]. The graphene nano powder with outer

diameter 10–20 micron and thickness 3–6 nm with purity of 96–99% was purchased from United Nanotech Innovations, Bengaluru, Karnataka, India. The Epoxidized Palm Oil (EPO) was prepared in the Advanced Tribology Lab, College of Engineering Trivandrum, Kerala, India. Teflon sheet of thickness 0.5 mm to prevent adhering of composite to the mould was supplied by vendor from Bangalore, Karnataka, India. Chloroform with a concentration of 99% used as the solvent and Sodium Hydroxide (NaOH) used for chemical treatment were supplied by Nice Chemicals Private Ltd, Kochi, Kerala, India. Mould with dimensions 310 × 260 × 4 mm (Mild Steel Plates) for hot compressing the composites and Mild Steel Trays of dimensions 310 × 260 × 20 mm for prepreg preparation were fabricated at Government Engineering College Barton Hill, Thiruvananthapuram, Kerala, India.

## 2.2 Alkaline treatment

Alkali treatment, commonly referred to as mercerization, is one of the oldest and most widely employed chemical processes for treating natural fibers. In the case of flax fiber mats, the procedure involved immersing them entirely in a 2% NaOH (sodium hydroxide) solution for a duration of 30 min as shown in Fig. 1. Subsequently, the flax fiber mats were removed from the solution and rinsed with a mild acid to eliminate any remaining unreacted alkali. To conclude the process, the mats were thoroughly washed with water multiple times and then left to dry in an air oven. Water absorption tests were carried out on flax fabrics and in laminate samples (before and after treatment) to ensure the enhancement of hydrophobic nature.

## 2.3 Epoxidation of palm oil (EPO)

Epoxidation is a chemical modification technique that involves replacing double bonds in alkenes with epoxide or oxirane rings. This process is achieved by using peracids, which are generated in situ through the combination of hydrogen peroxide ( $H_2O_2$ ) and a carboxylic acid like acetic acid or formic acid. Enzymes, metal catalysts, or ion exchange resins can be employed to facilitate this reaction. It is worth noting that epoxides are valuable intermediates in the synthesis of various products [31].

To perform this reaction, 600 ml of palm oil (PO) is mixed with 4 ml of glacial acetic acid, 20 ml of hydrogen peroxide, and a few drops of sulfuric acid. The mixture is then stirred using a magnetic stirrer for approximately 4.5 h within a temperature range of 60–70 °C. Afterward, the product is purified through a methanol wash. The kinematic viscosity is measured in accordance with ASTM D446 using Cannon–Fenske opaque viscometer shown in Fig. 2.

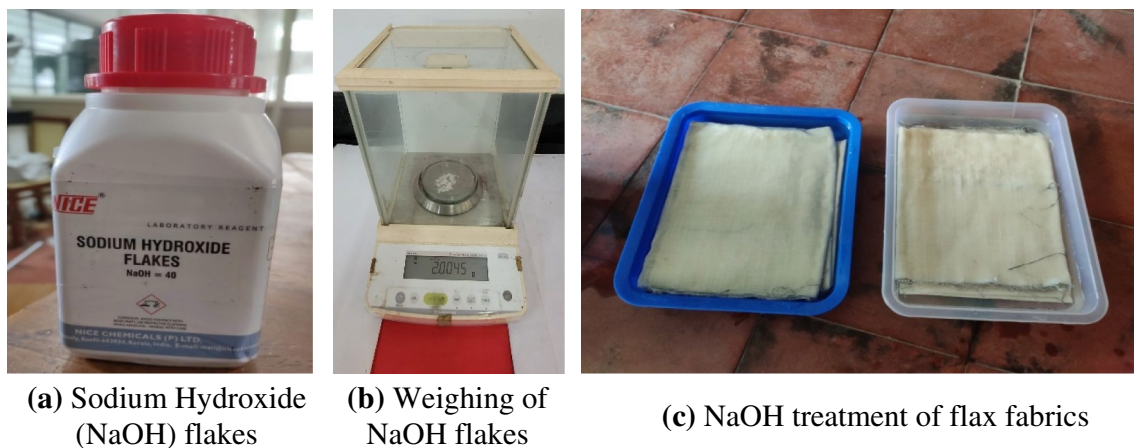


Fig. 1 Flax fiber treatment using 2% NaOH solution

**Fig. 2** Cannon Fenske opaque viscometer to measure the viscosity of PO and EPO



## 2.4 Solvent casting

In solvent casting process shown in Fig. 3, thermoplastic polymer films are formed by dissolving the polymer in a solvent, and this solution is used to form a film of the desired shape by using a mould. The polymer and solvent are the main components of this system, but additives are also added. The main advantages of this method are better uniformity in the thickness of layers, good flexibility, and better physical properties. As reported [18], the strength of the composite is improved after the solution casting due to the improvement in fiber impregnation and wettability. Moreover, the lack of thermal distortion maintains the fiber strength at higher values.

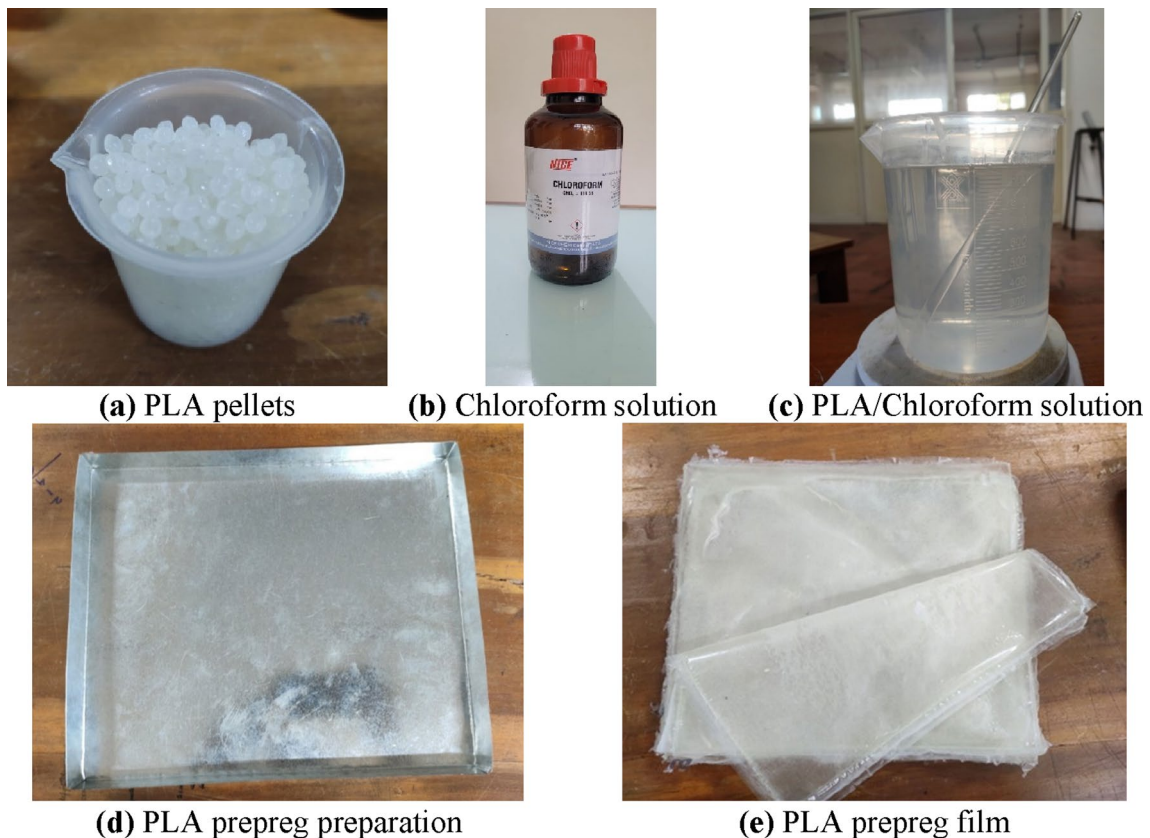
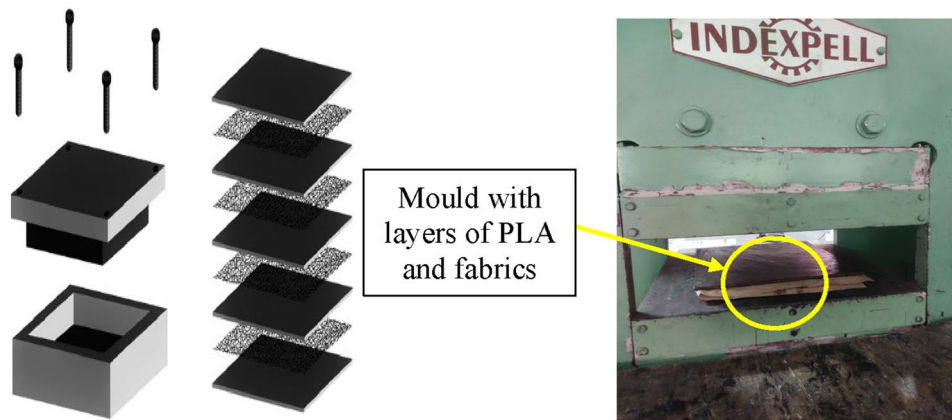


**Fig. 3** Solvent casting process



(a) Pictorial representation of layer sequence

(b) Hot compression to produce laminates

Fig. 4 Laminate preparation

Table 1 Types of fabricated laminates

Sl. no	Laminate	Sample code	Combinations
1	Laminate 1	FLAX/PLA	PLA/flax fiber fabric
2	Laminate 2	FLAX/PLA/EPO	PLA/flax fiber fabric with EPO
3	Laminate 3	FLAX/PLA/EPO/GN	PLA/flax fiber fabric with EPO and graphene nano particles

## 2.5 Hot press compression moulding method

In this process (Fig. 4), the preheated moulding material above the melting point, formed and cooled in the form of sheets, are kept open in a preheated mould cavity. This material is compressed for a known pressure after closing the mould with a top member. Here, it is made sure that the applied pressure is uniformly distributed to all areas until the moulding material has cured, compression moulding. In this process, the design parameters are the moulding time, temperature, and pressure [32].

## 2.6 Fabrication of composite laminates

The fabrication of three different type of composite laminates shown in Table 1 are explained below.

### 2.6.1 FLAX/PLA composite

Green composites are manufactured by solution casting technique by dissolving PLA pellets in chloroform (solvent) in the ratio 10:1(v/w) and the prepared prepregs were hot compressed, shown in Fig. 5. Here PLA prepreg sheets were prepared by dissolving PLA pellets in a known volume (1 L) of chloroform by properly stirring for a known time (2 h) and poured into an MS tray of dimensions  $310 \times 260 \times 20$  mm. These PLA sheets are allowed to cure by keeping them open for 24 h at room temperature, and any chloroform present will evaporate.

Flax fiber/PLA sheets were meticulously crafted through a method involving the careful pouring of a solution composed of PLA and chloroform into a tray made of MS (mild steel) with matching dimensions. In the process, a Flax fiber fabric measuring  $310 \times 260$  mm was strategically positioned on the PLA/chloroform solution. Subsequently, a modest quantity of PLA/chloroform solution was gently poured over the Flax fiber fabric, and the entire assembly was left undisturbed for a duration of 24 h, allowing the chloroform to evaporate. This procedure was iteratively applied to produce

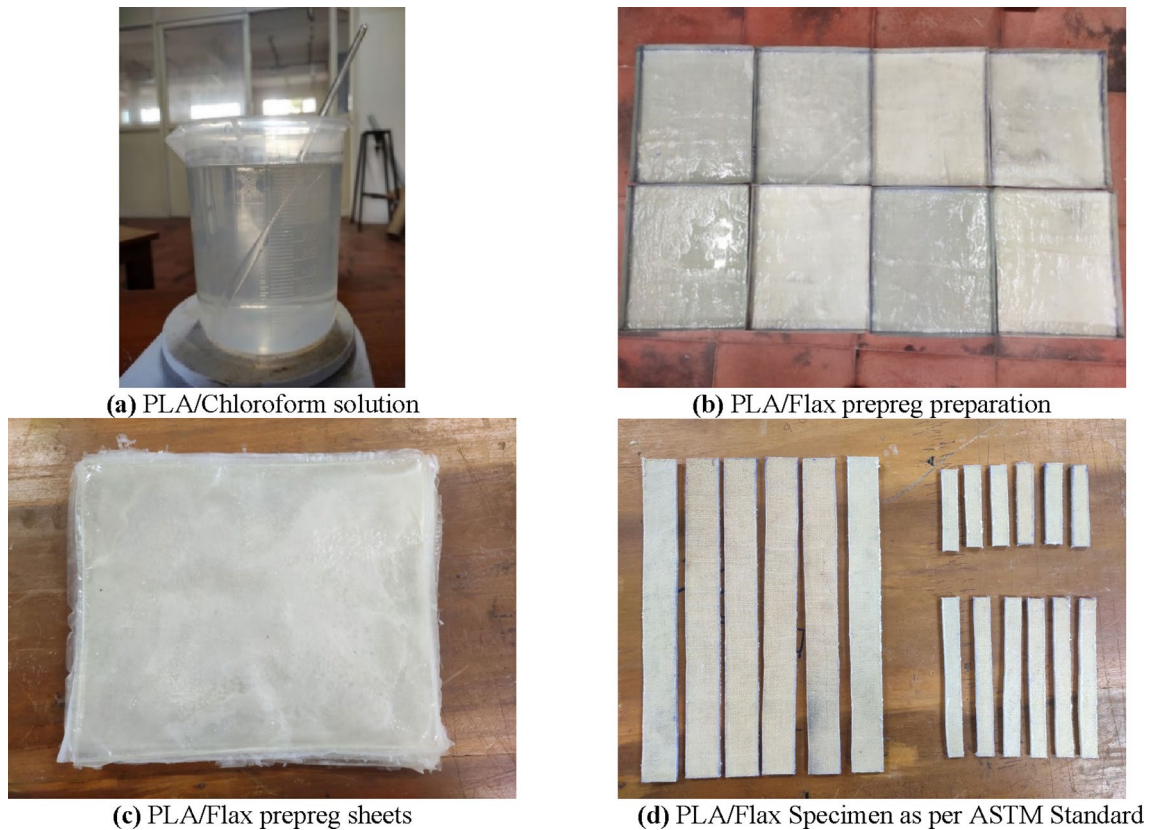


**Fig. 5** FLAX/PLA composite preparation

a total of five layers of PLA sheets, alternated with four layers of Flax fiber/PLA prepreg sheets. This meticulous layering approach was employed to create a composite material with desirable characteristics, blending the properties of PLA and Flax fiber for enhanced performance.

A decrease in composite performance with an increase in temperature (from 230 to 250 °C) and process time (from 2 to 5 min) was reported [33]. Here these overlapped sheets are hot compressed at a pressure of 5 MPa at 180 °C temperature for 15 min and later allowed to cure by keeping it at room temperature for 6 h. After curing, these samples are made to ASTM testing standards. Teflon sheets and silicon grease were used to avoid sticking the matrix in the mould during hot compression.

### 2.6.2 FLAX/PLA composite with EPO

A known amount of PLA pellets and chloroform solvent were taken in a volume beaker in the ratio 10:1 (v/w). The PLA gets dissolved in the chloroform on stirring over a mechanical stirrer for about 2 h at a slow speed.

After the solubilization of PLA, about 5 wt% EPO was added and stirred for another 1 h to form a better PLA/EPO blend solution. The methodology used for manufacturing FLAX/PLA Composite is also used here for FLAX/PLA/EPO Composite shown in Fig. 6.

### 2.6.3 FLAX/PLA composite with EPO and graphene nano filler

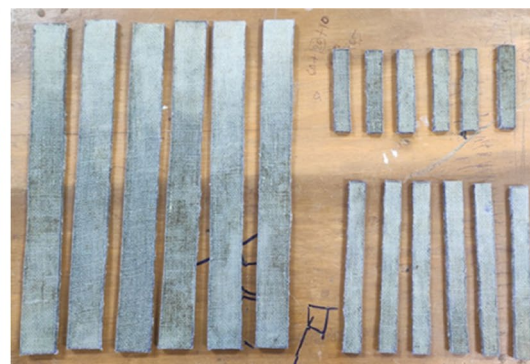
A known amount of PLA pellets were dissolved in the chloroform solvent taken in a volume beaker in the ratio 10:1 (v/w). The PLA gets dissolved in the chloroform on stirring over a mechanical stirrer for about 2 h [34].

After the solubilization of PLA, EPO of about 5 wt% was added and stirred for another 1 h to form a better PLA/EPO blend solution. At the same time, 0.5% graphene powder was added to 20 ml chloroform and ultrasonicated in an ice-water bath for 30 min. The graphene/Chloroform solution is then added drop by drop into the PLA/EPO/Chloroform solution and is stirred for a period of 1 h. Followed by this, PLA/EPO/graphene blend films were prepared

**(a)** PLA/EPO/Chloroform Solution**(b)** FLAX/PLA/EPO composite specimen as per ASTM Standard**Fig. 6** FLAX/PLA/EPO composite preparation

by pouring a small amount of PLA/EPO/graphene/chloroform solution into an MS tray. The setup was then kept for 24 h at room temperature to evaporate chloroform.

Concurrently, FLAX/PLA/EPO/graphene blend films were meticulously crafted through a precise procedure. A solution comprising PLA/EPO/graphene/chloroform was skillfully poured into a tray constructed from mild steel (MS). Positioned atop this PLA/EPO/graphene/chloroform solution was a Flax fabric measuring  $310 \times 260$  mm. Subsequently, a judicious amount of the PLA/EPO/graphene/chloroform solution was delicately poured over the Flax fabric, and the ensemble was allowed to undergo a 24-h period for the chloroform to evaporate. This meticulous process was iterated to yield five layers of PLA/EPO/graphene sheets, interspersed with four layers of FLAX/PLA/EPO/graphene prepreg sheets. The stratification of these sheets was carefully arranged within a mold, and this assembly was subjected to a hot compression molding machine. Compression was applied at a pressure of 5 MPa under a temperature of  $180^\circ\text{C}$  for a duration of 15 min. Subsequently, the composite laminate underwent a cooling phase at room temperature for 6 h. After the cooling process, various test samples were precisely cut in accordance with ASTM testing standards, as illustrated in Fig. 7. Teflon sheets and silicon grease were employed to prevent adhesion of the matrix to the mold during hot compression, ensuring a seamless fabrication process.

**(a)** Graphene solution after ultrasonication**(b)** PLA-EPO-graphene solution**(c)** PLA-EPO-Graphene/Flax Specimen as per ASTM Standard**Fig. 7** FLAX/PLA/EPO/graphene composite preparation

## 2.7 Physical characterization

### 2.7.1 Density analysis

The density of different PLA composite combinations was ascertained employing a high-precision digital weighing machine with an accuracy range of 0.0001 g adhering to ASTM D-792 standard. For each combination, five samples were meticulously prepared for the purpose of this test.

### 2.7.2 Determination of moisture content

The moisture content percentage was measured by using oven drying method by adopting ASTM D6980 standard in terms of loss in weight. The moisture content in the flax fabric and resulting flax fabric PLA based composites was determined by equation.

$$M(\%) = \frac{W_1 - W_2}{W_1} \times 100$$

The moisture content ( $M\%$ ) is expressed as a percentage, calculated by comparing the weights of the composite before ( $W_1$ ) and after ( $W_2$ ) wetting, where  $W_1$  and  $W_2$  are measured in grams. This process was systematically repeated across all samples of each composite, and the resulting density values were meticulously tabulated.

### 2.7.3 Dimensional stability

The analysis of dimensional stability encompassed a comprehensive examination of water absorption, thickness swelling and width swelling following the guidelines outlined in the ASTM D570-98 standard. Initial measurements of weight, thickness, and width were meticulously conducted using a precision weighing machine with an accuracy of 0.0001 g, along with a digital micrometer for the respective measurements of thickness and width. In this refined procedure, specimens from each of the three laminates were immersed in distilled water, consistently maintained at 21.5 °C, for various durations, with a maximum limit of 60 min. At predefined time intervals (15, 30 and 60 min), the samples were carefully removed from the water. Subsequent to extraction, any surface moisture was promptly eliminated, and the samples underwent meticulous measurements for weight, thickness, and width.

### 2.7.4 Porosity

Porosity analysis for PLA composite combinations was conducted by employing the water displacement method. Porosity, defined as the ratio of the absorbed volume to the total volume of the composite laminates, encompasses all pores, air pockets, and any cavities within the material.

## 2.8 Mechanical characterization of composites

### 2.8.1 Tensile test

The tensile strength of the laminates was assessed in accordance with the ASTM D3039 standard. The specimen was subjected to loading conditions designed to induce fracture in the anticipated region, with the occurrence of breakage contingent upon the localized stress distribution. The imperative for such loading protocols is rooted in the need for precise control over the fracture site to ensure accurate measurement of tensile strength. Mechanics behind the composite failure modes are explained in detail [35]. The specimen dimensions were taken as 250 × 25 × 4 mm. The specimen's ends were securely fastened between the jaws. Tensile force was applied to the specimen through controlled movement of the jaws, and this force was meticulously documented in relation to the alterations in gauge length. The tensile testing procedure was conducted using a Computerized Universal Testing Machine., specifically



**Fig. 8** Experimental setup of tensile test specimen with extensometer

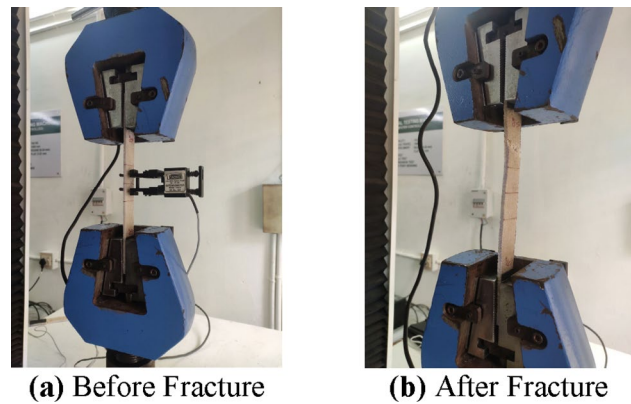
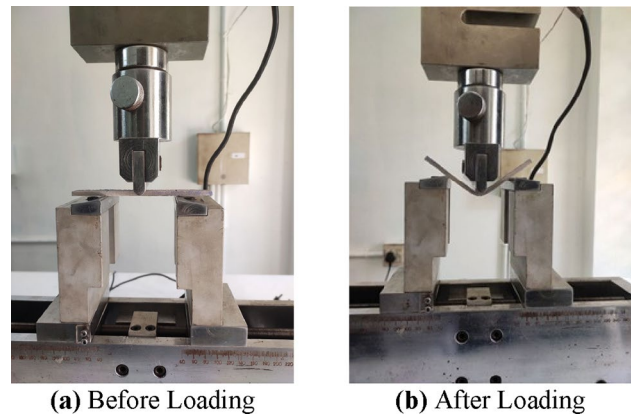


**Fig. 9** Flexural test specimen with the experimental setup



the KIC-2-1000-C model, which boasts a maximum load capacity of 100 kN. The specimens underwent testing at a controlled loading rate of 2 mm/min to ensure precision in the evaluation process.

Samples extracted from three distinct laminate types underwent tensile testing, with five specimens tested per laminate to establish average values. Figure 8 illustrates the experimental setup for the tensile test specimens across various laminates. Numerous researchers, as cited in references [36, 37] have underscored the pivotal role of stacking sequence in influencing the tensile properties of composites. Various factors impact the tensile response, including the choice of materials, methods of material preparation, stacking sequence of fiber layers, specimen preparation techniques, specimen conditioning, testing environment, testing speed, void content, and notably, the fiber weight fraction. It's noteworthy that the extensometer utilized in this study features a gauge length of 25 mm.

### 2.8.2 Flexural test

The evaluation of the specimen's flexural strength involved applying both tensile and compressive stresses along its midsection. This testing procedure was conducted utilizing a Computerized Universal Testing Machine, specifically the KALPAK UTM (Model No. KIC-2-1000-C), boasting a maximum load capacity of 100 kN. The specimens, adhering to the ASTM D790 test standard, were crafted with dimensions of  $127 \times 12.7 \times 4$  mm. To maintain consistency with ASTM D790 guidelines, a standardized span length of 64 mm, in a ratio of 16:1, was employed. The bending forces applied during testing were measured to gauge the specimen's structural integrity and performance under tensile and compressive loads.

Three-point bending test was performed with an applied load of 2 mm/min until the specimen fractures and broke. The experimental set up of flexural test specimen before and after bending is shown in Fig. 9. Here in the test specimen, both compressive and tensile stress will be acting simultaneously. The maximum load is recorded at specimen failure; from the recorded maximum load, the values for modulus of elasticity was evaluated.

**Fig. 10** Izod impact specimen with the experimental setup

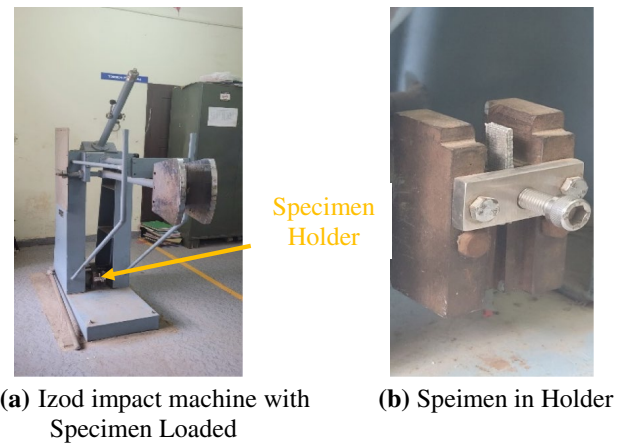
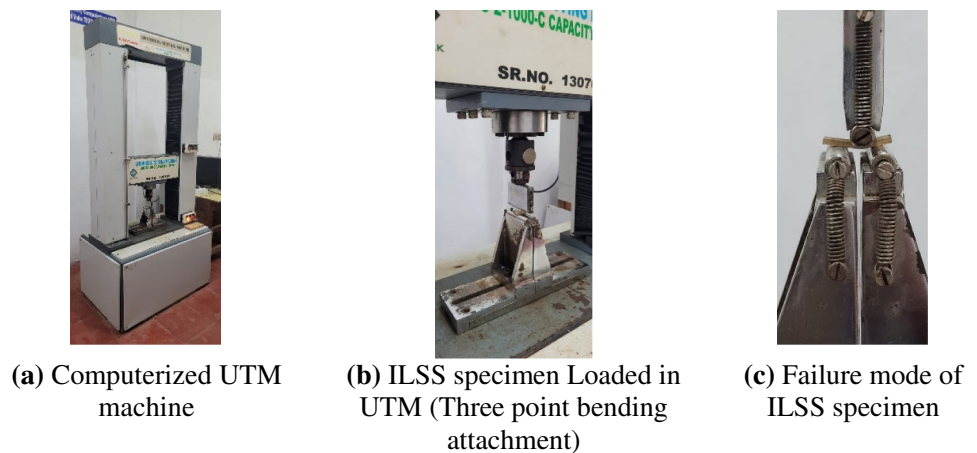


**Fig. 11** ILSS specimen with the experimental setup



### 2.8.3 Impact test

The specimens of size  $64 \times 12.7 \times 4$  mm conforming to ASTM D256 standard are tested for impact strength using an Izod impact test rig; from the impact made by the pendulum on the specimen, the impact energy required for crack initiation to the same for breakage of the specimen is plotted. Figure 10 shows the test specimens with set up used for the Izod impact test.

### 2.8.4 Short beam test

Unlike other materials, the complex structure of composites makes the internal stress nature also complicated. Here the matrix, the resin, and interlaminar properties have a critical role to play in the failure modes. Here a small ratio of width to span (1:3) as per ASTM D2344 has been taken for performing the ILSS test.

The interlaminar shear strength (Short beam strength) is obtained by using the Eq. 1 [38].

$$F_{sbs} = 0.75 \frac{P}{bh} \text{ (MPa)} \quad (1)$$

where  $p$  = maximum Load observed during the test (N),  $b$  = width (mm),  $h$  = thickness (mm).

The ILSS specimens with experimental setup are shown in Fig. 11.

### 2.8.5 Scanning electron microscopy

The fracture surfaces of tensile test specimens of FLAX/PLA, FLAX/PLA/EPO and FLAX/PLA/EPO/Graphene specimens were observed by scanning electron microscopy (SEM) of model TESCAN VEGA 3 LMU high-performance, Variable Pressure

Analytical SEM with LAB6 having high resolution of 2 nm, along with the most advanced LN2-free high-resolution. Prior to the analysis, the specimens were coated with a thin layer of gold to get good conductivity, using a Quorum SC7620 sputter coater.

### 3 Results and discussion

#### 3.1 Physical characterization

##### 3.1.1 Density analysis

**3.1.1.1 Flax fiber fabric** Density of flax fibre fabric before and after treatment (Alkalization) was measured and is tabulated in the Table 2. It is seen that the density of alkaline treated fabric has a marginal increase of value from 0.45 to 0.47 kg/m<sup>3</sup>. This can be attributed to the fact that hydroxyl groups are replaced with sodium ions, moreover the sodium ions has got a favourable diameter, able to widen the smallest pores in between the lattice planes and penetrate into them, there by increase in density.

**3.1.1.2 Flax fiber composites** The assessment of densities across various PLA composite combinations has yielded results outlined in Table 2. Specifically noteworthy is the 19% decrease in the density of FLAX/PLA/EPO laminate. This decline is ascribed to the introduction of EPO into the composite, a factor that instigates the formation of microvoids within the material. These outcomes align coherently with the observations from morphological analysis. On the contrary, the introduction of graphene has showcased a positive influence on density, evident in the filling of voids. This augmentation in density values facilitates superior adhesion within the matrix and the fibers.

##### 3.1.2 Determination of moisture content

**3.1.2.1 Flax fiber fabric** The moisture content of flax fibre fabric was determined and tabulated in Table 2. It is seen that the moisture content values has decreased from 9.53 to 6.31%. This clearly indicates that fabric after alkaline treatment has turned to more hydrophobic due the fact that the hydroxyl groups present in the structure of flax has been replaced with sodium ions.

**3.1.2.2 Flax fiber composites** The findings regarding the moisture content variation in the composites parallel those observed in density. Specifically, the moisture content of FLAX/PLA/EPO has exhibited an increase, attributed to the promotion of capillary action facilitated by the presence of microvoids. Upon the introduction of graphene nanoparticles in the FLAX/PLA/EPO/Graphene composite, these molecules effectively occupy the microvoids, leading to a notable reduction in moisture content to 3.46%. The corresponding moisture content values are detailed in Table 2.

##### 3.1.3 Dimensional stability

The assessment of dimensional stability involved a thorough investigation, encompassing water absorption, thickness swelling and width swelling, in adherence to the ASTM D570-98 standard. The results obtained from these assessments

**Table 2** Experimental results of physical tests conducted on composite laminates

	Specimen code	Density Kg/m <sup>3</sup>	Water absorption (%)			Thickness swell %	Width swell %	Moisture content (%)	Porosity (%)
			15	30	60				
Fabric	FLAX	0.45	78.69	72.96	69.97	–	–	9.53	–
	FLAX/NaOH	0.47	72.38	66.18	64.98	–	–	6.31	–
Laminate	FLAX/PLA (L1)	0.86	9.53	5.93	4.43	0.83	0.75	5.63	3.98
	FLAX/PLA/EPO (L2)	0.69	10.91	10.83	10.09	0.97	0.89	5.80	7.13
	FLAX/PLA/EPO/GN (L3)	0.91	7.59	4.25	3.29	0.35	0.33	3.47	2.40

**Fig. 12** Variation of kinematic viscosity: before and after epoxidization on Palm oil

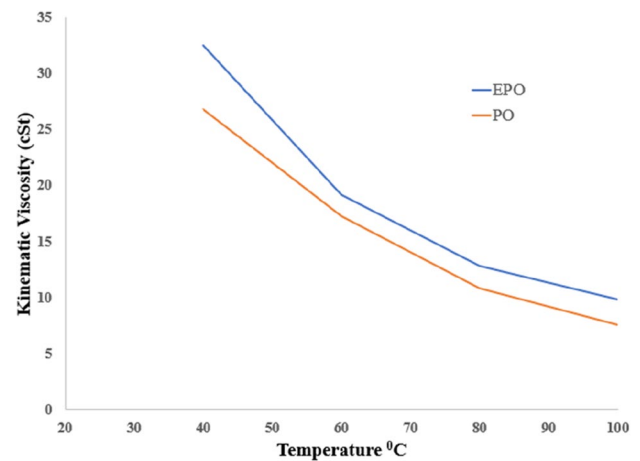


**Table 3** Mechanical properties of flax fiber reinforced composites (experimental results)

Laminate	Tensile strength (MPa)	Tensile modulus (GPa)	Flexural strength (MPa)	Flexural modulus (GPa)	Impact energy (J/m)	Short beam strength (MPa)
FLAX/PLA (L1)	23.20	2.55	121.86	2.9	40.35	31.25
FLAX/PLA/EPO (L2)	20.30	1.25	90.35	1.3	33.58	21.65
FLAX/PLA/EPO/GN (L3)	26.45	3.20	132.56	3.8	43.69	35.85

are presented in Table 2. For flax fiber fabric with alkalization treatment, the fall in water absorption values can be attributed to the replacement of hydroxyl groups with sodium.

In the case of composites, the increase in water absorption values for FLAX/PLA/EPO is linked to the presence of microvoids, causing slight disturbances in dimensional stability reflected in marginal increases in thickness and width values. Notably, for FLAX/PLA/EPO/Graphene composite, a decrease in water absorption values is observed. This can be attributed to graphene occupying the voids, thereby enhancing adhesion within the matrix and fibers. Consequently, this contributes to stabilized dimensional stability, evident in negligible variations in thickness and width.

### 3.1.4 Porosity

Porosity values obtained for FLAX/PLA, FLAX/PLA/EPO and FLAX/PLA/EPO /Graphene specimens follows the same pattern for other scenario, where FLAX/PLA/EPO has higher porosity values owing to the microvoids. As the addition of graphene the porosity values has decreased to 2.4%, which shows the compactness of composite with better adhesion between all the constituents.

## 3.2 Viscosity measurement

To measure kinematic viscosity in accordance with ASTM D446, a Cannon–Fenske opaque viscometer is employed. The procedure involves immersing the sample in a temperature-controlled viscometer bath. When the oil within the viscometer reaches the desired temperature, it needs to be marked. This marking process requires measuring both the time it takes and the viscosity at this point. Subsequently, the recorded marking is multiplied by a specific factor to convert it into centistokes, yielding the kinematic viscosity value.

Viscosity tests were conducted for both regular palm oil and epoxidized palm oil, and the results are depicted in Fig. 12. The findings reveal that the viscosity of epoxidized palm oil has increased, primarily due to the chemical changes resulting from epoxidation, which have led to enhanced intermolecular interactions. The heightened polarity of epoxides, being more polar in nature, likely also plays a role in this viscosity increase. This augmented viscosity is a significant factor contributing to the enhanced ductility of the laminate composite.

### 3.3 Tensile properties

A detailed study of flax fiber-based composites with different combinations was carried out for this, and the results were shown in Table 3. The tensile properties of the laminates were measured by using the ASTM D3039 standard. In this study, as mentioned earlier, a Computerized Universal Testing Machine (Make: KALPAK UTM, Model No. KIC-2-1000-C with a maximum load capacity of 100 kN). The specimen clamped is of dimension  $250 \times 25 \times 4$  mm, and the ends of the specimen have been clamped between the jaws so that the breakage is occurring in the expected region. The tensile force on the specimen was recorded with respect to the change in gauge length at a loading rate of 2 mm/min. The specimen, which was cut from three different types of laminates, was subjected to a tensile test for five samples per laminate to get an average value, which is shown in Fig. 13.

The extensometer used here has a gauge length of 25 mm, and the values obtained for induced stress and strain are plotted and shown in Fig. 13. The initial linear portion of the curve accounted for the elastic behavior, and the variation from the linear portion is due to the initiation of a crack in the matrix and also accounted for the start of fiber failure.

As the loading continued, the crack also propagated, leading to the failure of fracture of fiber and resulting in fiber failure; the value corresponds to ultimate stress. The ultimate stress value obtained for laminate 1 (FLAX/PLA) composite is 23.20 MPa, which is high for the same combination composite for fiber 18.80 MPa as reported in the literature [25]. The ultimate stress value is attributed to the increased strength due to the interlocking effect of the woven structure of the fabric [15]. The polar oxygen atoms present in the Poly Lactic Acid (PLA), used as the resin here, react to the hydroxyl groups in the flax fiber to form hydrogen bonds, which in turn create strong bonding [18]. Some studies reported that non-woven natural fiber reinforced composites provides lesser tensile strength as compared to woven mats [39]. Even though a wide range of values starts from 21 Mpa [40] to 110 Mpa [41] for tensile strength for the laminate 1 composites has been reported, the value obtained as shown in Table 2 for the same composition here of 23.20 MPa falls within the range, also an observed value of 2.55 GPa for Young's Modulus, hence the test procedure is justified. Even though the laminate 1 has high strength but it is highly brittle due to the presence of PLA; furthermore, laminate 1 is of slow degradation rate.

In order to overcome these limitations, laminate 2 (FLAX/PLA/EPO) was prepared by adding 5% EPO to laminate 1. As already reported [42] that the addition of chemical reaction epoxidized palm oil (EPO) in rubber composites, has increased mechanical properties, including lowering of brittle nature. Laminate 2 was tested to tensile strength, and the value was found to be 20.30 MPa and Young's modulus value of 1.25 GPa. Even though the tensile strength and Young's modulus values were found to be less when compared with laminate 1, there has been a considerable increase in the ductility of the composite. It was also noted that there is a change in viscosity due to the addition of EPO contributes to the laminate being more flexible.

Even though the ductility of composite has increased considerably in laminate 2 by the addition of EPO but only with a compromise to the tensile strength, which reduces the industry application range; hence the strength needs to be enhanced. For this 0.5% graphene has been added to the laminate 2 combinations, hence laminate 3 (FLAX/PLA/EPO/GN). It is seen that there is a considerable increase in the mechanical properties of laminate 3, especially in the case of tensile strength. For laminate 3 the maximum tensile strength value obtained is 26.45 MPa, and Young's modulus value of 3.20 GPa. The reason for this is attributed to the better dispersion and spread of the graphene nanoparticle [27]. For revealing this phenomena, SEM images were taken, and analysis will be followed in a later section. In short, from the

Fig. 13 Stress-strain variation of composite laminates

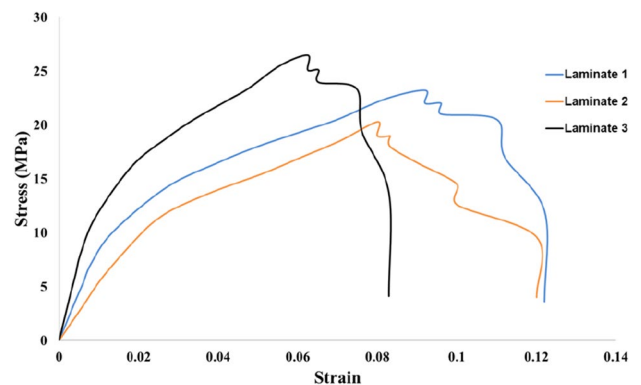


**Fig. 14** Plot of flexural stress variation of different laminate

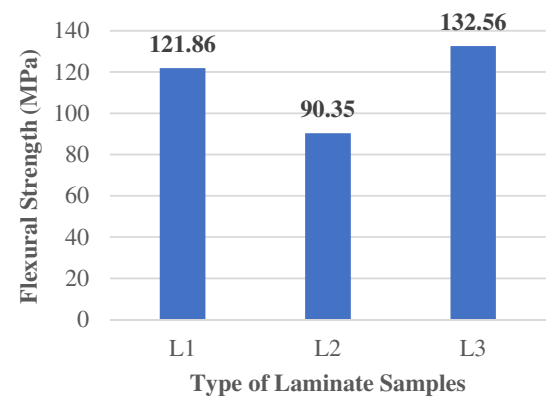
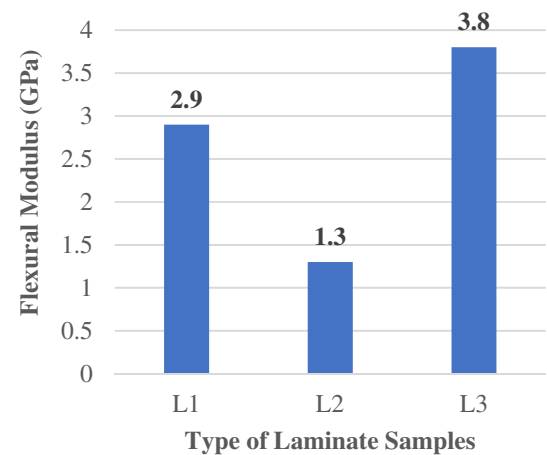


**Fig. 15** Plot of flexural modulus variation of different laminate



tensile test results, it is evident that by the addition of EPO, there was a significant increase in ductility at the expense of tensile strength, as seen in laminate 2, which was compensated by the addition of graphene.

### 3.4 Flexural properties

Similar to the tensile test three-point bending test for laminates was carried out in Computerized Universal Testing Machine (Make: KALPAK UTM, Model No. KIC-2-1000-C with a maximum load capacity of 100 kN) as per ASTM test standard D 790-10. Owing to the bending theory, the strain rate for the outer layer of the laminates was tested in displacement control mode at a constant crosshead speed of 5 mm/min. The span length for the three-point flexural test was selected as 64 mm according to the specimen thickness.

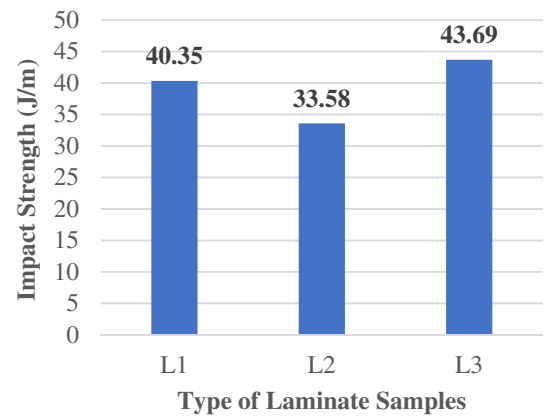
The results obtained for the flexural test are recorded in Table 3, and it is seen that flexural strength values follow the same trend as that of the tensile test. The current study showed that the fabricated composite possesses enough flexural strength for this application. A graph with variation of flexural stress and modulus was also plotted, as shown in Figs. 14 and 15.

Throughout the testing process, no specimen experienced failure due to delamination, and there was minimal to no evidence of fiber pull-out in the observed failure modes. Fracture consistently initiated on the tension side of the beam, with the point of fracture consistently situated in the middle of the specimen. Typically, the modulus is highly sensitive to the interfacial bonding between the matrix and fibers. For Laminate 1, the average values for ultimate flexural strength and flexural modulus were determined to be 121.86 MPa and 2.9 GPa, respectively. Corresponding values for Laminates 2 and 3 were found to be 90.35 MPa, 1.3 GPa, and 132.56 MPa, 3.8 GPa, as presented in Table 3.

### 3.5 Impact properties

The specimens of laminates 1, 2 & 3 conforming to ASTM D256 standard dimensions were tested for impact strength using an Izod impact test rig and are plotted in Fig. 16.

**Fig. 16** Plot of variation of impact strength of laminates



The average impact strength, as detailed in Table 3 for Laminate 1, 2, and 3, stands at 40.35 J/m, 33.58 J/m, and 43.69 J/m, respectively. These outcomes mirror the trends observed in both the tensile and flexural tests. The recorded impact strength of 40.35 J/m for Laminate 1 aligns with existing literature. The diminished impact strength in Laminate 2 is ascribed to the penetration of the EPO into the matrix structure, its presence in the interfacial area, and the intermolecular interactions induced by the PLA. Conversely, the improved dispersion and uniformity of graphene nanoparticles contribute to the heightened impact strength values observed in Laminate 3 (FLAX/PLA/EPO/GN).

### 3.6 Short beam test (inter laminar shear strength (ILSS))

The short beam test for determining the interlaminar shear strength of laminates was carried out using a three-point bending test, as mentioned in the previous section. The specimen made of laminates was aligned to ASTM D 2344-06 standards by keeping the ratio of length to thickness as 6:1 and width to thickness ratio as 2:1.

The values obtained as shown in Fig. 17 for short beam strength of laminates 1, 2, and 3 were 31.25 MPa, 21.65 MPa and 35.85 MPa respectively. Even though all the laminates failed during the test due to delamination, the short beam strength values obtained followed the same pattern as that of the tensile, flexural, and impact strength, with maximum value for short beam strength obtained for laminate 3 (FLAX/PLA/EPO/GN) due to the even spread and better dispersion of graphite nanoparticles.

The summary of the mechanical properties obtained for all three laminates for various test are given in Table 3.

### 3.7 Scanning electron microscopy (SEM) analysis

SEM images to observe the surface morphology at the rupture part of the tensile samples of the laminates 1, 2, and 3 were taken and are shown in Figs. 18, 19 and 20.

**Fig. 17** Inter laminar short beam shear strength for different laminates

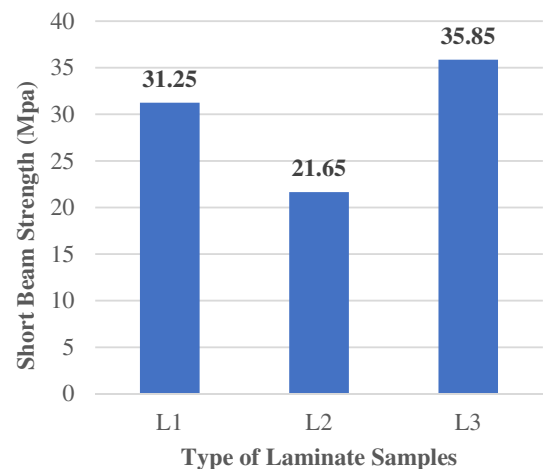


**Fig. 18** Fractured surface of PLA/FLAX laminate

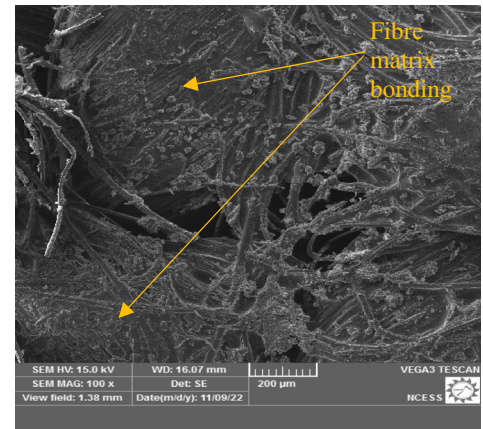


**Fig. 19** Fractured surface of PLA/EPO/FLAX laminate

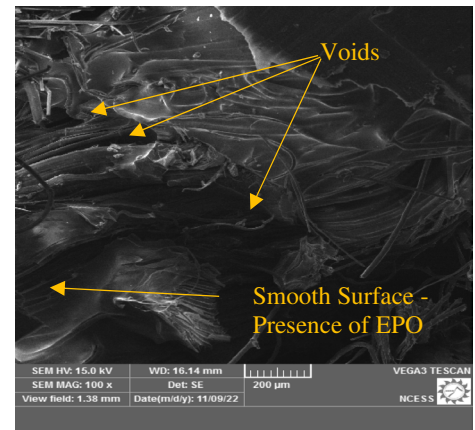
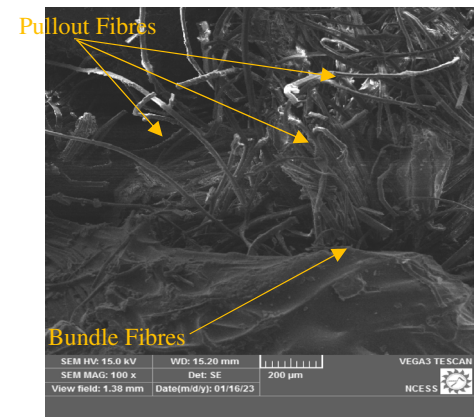


**Fig. 20** Fractured surface of PLA/EPO/graphene/FLAX laminate



The images show the damage caused to the matrix due to the tensile loading; it also shows the penetration of resin into the reinforcements and filling the voids, thereby creating good bonding between both. The presence of bundled fibers in the laminates 1 and 3 indicates good adhesion within the matrix and the fibers. The presence of micro voids in laminate 2 attributed to the reduction in strength, as reported in all the tests. However, the clear image of good dispersion with strong bonding between the layers of fibers and matrix shown in the laminate 3 supports the higher mechanical properties obtained in all the tests performed.



## 4 Conclusions

The recent advancements in composite manufacturing technology have ushered in a new era of sustainable engineering, prominently represented by the widespread adoption of natural fiber composites, with flax fiber standing out as a key player. The pivotal aspect of this development lies in the formulation of an environmentally friendly composite, achieved through the amalgamation of alkali-treated flax fiber reinforcement and a poly lactic acid (PLA) polymer matrix via a hot compression technique. The investigation into water absorption has unveiled the transformative effects of alkaline treatment on flax fibers, enhancing their hydrophobic nature and crystallinity. This enhancement, in turn, fosters improved adhesion between the flax fiber reinforcement and the polymer matrix. The introduction of 5% wt of epoxidized palm oil (EPO) as plasticizers not only addresses issues of brittleness but also contributes to an elevation in thermal stability. Taking innovation a step further, the incorporation of 0.5 wt% of graphene nanoparticles as nano-fillers has resulted in a composite material with superior mechanical properties. This research places a significant emphasis on the thorough mechanical characterization of these green composites, encompassing tensile, flexural, and impact properties, as well as an assessment of inter-laminar shear strength. Furthermore, a meticulous analysis of dimensional stability has been conducted, shedding light on the environmental performance of the developed composites. Morphological scrutiny using scanning electron microscopy provides valuable insights into the structural aspects of the composite materials. The integration of flax fibers, alkaline treatment, epoxidized palm oil, and graphene nanoparticles demonstrates a holistic approach towards achieving both ecological and engineering excellence.

**Acknowledgements** Author gratefully acknowledges the support of National Institute of Rubber Training (NIRT), Kottayam for allowed to use Hot Press Compression Moulding Machine in making biodegradable green composite laminates.

**Author contributions** NJ spearheaded the conceptualization and design of the analysis, played a pivotal role in data collection, conducted experiments, performed comprehensive data analysis, and took the lead in crafting the manuscript. IS was instrumental in conceptualizing and designing the analysis, executing experiments, conducting data analysis, and actively contributing to the manuscript's development. KBK contributed significantly to the conceptualization and design of the analysis, played a key role in both data collection and experimentation, conducted thorough data analysis, and made substantial contributions to the manuscript's creation.

**Data availability** The datasets generated during and/or analysed during the current study are available from the corresponding author on reasonable request.

## Declarations

**Competing interests** The authors declare no competing interests.

**Open Access** This article is licensed under a Creative Commons Attribution 4.0 International License, which permits use, sharing, adaptation, distribution and reproduction in any medium or format, as long as you give appropriate credit to the original author(s) and the source, provide a link to the Creative Commons licence, and indicate if changes were made. The images or other third party material in this article are included in the article's Creative Commons licence, unless indicated otherwise in a credit line to the material. If material is not included in the article's Creative Commons licence and your intended use is not permitted by statutory regulation or exceeds the permitted use, you will need to obtain permission directly from the copyright holder. To view a copy of this licence, visit <http://creativecommons.org/licenses/by/4.0/>.

## References

1. Liu W, Chen T, Fei M, Qiu R, Yu D, Fu T, et al. Properties of natural fiber-reinforced biobased thermoset biocomposites: effects of fiber type and resin composition. *Compos B Eng*. 2019;171:87–95. <https://doi.org/10.1016/j.compositesb.2019.04.048>.
2. Bax B, Müssig J. Impact and tensile properties of PLA/cordenka and PLA/flax composites. *Compos Sci Technol*. 2008;68(7):1601–7. <https://doi.org/10.1016/j.compscitech.2008.01.004>.
3. Ye X, Gao Q, Yang P, Yang C, He E, Ye Y, et al. Mechanical and microwave absorbing properties of graphene/Mn–Zn ferrite/polylactic acid composites formed by fused deposition modeling. *J Mater Sci*. 2023;58(6):2525–38. <https://doi.org/10.1007/s10853-023-08196-x>.
4. Mayilswamy N, Kandasubramanian B. Green composites prepared from soy protein, polylactic acid (PLA), starch, cellulose, chitin: a review. *Emergent Mater*. 2022. <https://doi.org/10.1007/s42247-022-00354-2>.
5. Ebrahimnezhad-Khaljiri H, Eslami-Farsani R, Najafi M, Saeedi A. Introduction to epoxy/natural fiber composites. In: *Handbook of epoxy/fiber composites*. Springer; 2022. p. 485–514. [https://doi.org/10.1007/978-981-19-3603-6\\_19](https://doi.org/10.1007/978-981-19-3603-6_19)
6. Jeyapragash R, Srinivasan V, Sathiyamurthy S. Mechanical properties of natural fiber/particulate reinforced epoxy composites—a review of the literature. *Mater Today Proc*. 2020;22:1223–7. <https://doi.org/10.1016/j.matpr.2019.06.655>.

7. Sreekumar PA, Thomas S. 2—matrices for natural-fibre reinforced composites. In: Pickering KL, editor. Properties and performance of natural-fibre composites. Sawston: Woodhead Publishing; 2008. p. 67–126. <https://doi.org/10.1533/9781845694593.1.67>.
8. Sun Y, Zheng Z, Wang Y, Yang B, Wang J, Mu W. PLA composites reinforced with rice residues or glass fiber—a review of mechanical properties, thermal properties, and biodegradation properties. *J Polymer Res.* 2022;29(10):422. <https://doi.org/10.1007/s10965-022-03274-1>.
9. Mirzamohammadi S, Eslami-Farsani R, Ebrahimnezhad-Khaljiri H. The experimental assessment of carbon nanotubes incorporation on the tensile and impact properties of fiber metal laminate fabricated by jute/basalt fabrics-aluminum layers: As hybrid structures. *Proc Inst Mech Eng C J Mech Eng Sci.* 2023;237(8):1877–86. <https://doi.org/10.1177/09544062221134223>.
10. Mirzamohammadi S, Eslami-Farsani R, Ebrahimnezhad-Khaljiri H. The characterization of the flexural and shear performances of laminated aluminum/jute–basalt fibers epoxy composites containing carbon nanotubes: As multi-scale hybrid structures. *Thin-Walled Struct.* 2022;179:109690. <https://doi.org/10.1016/j.tws.2022.109690>.
11. Kandola BK, Mistik S, Pornwannachai W, Anand S. Natural fibre-reinforced thermoplastic composites from woven-nonwoven textile preforms: mechanical and fire performance study. *Compos B Eng.* 2018;153:456–64. <https://doi.org/10.1016/j.compositesb.2018.09.013>.
12. Nurul Fazita M, Jayaraman K, Bhattacharyya D, Mohamad Haafiz M, Saurabh CK, Hussin MH, et al. Green composites made of bamboo fabric and poly(lactic) acid for packaging applications—a review. *Materials.* 2016;9(6):435. <https://doi.org/10.3390/ma9060435>.
13. Morales J, Michell RM, Sommer-Márquez A, Rodrigue D. Effect of biobased SiO<sub>2</sub> on the morphological, thermal, mechanical, rheological, and permeability properties of PLLA/PEG/SiO<sub>2</sub> biocomposites. *J Compos Sci.* 2023;7(4):150. <https://doi.org/10.3390/jcs7040150>.
14. Srinivasan VS, Rajendra Boopathy S, Sangeetha D, Vijaya RB. Evaluation of mechanical and thermal properties of banana-flax based natural fibre composite. *Mater Des.* 2014;60:620–7. <https://doi.org/10.1016/j.matdes.2014.03.014>.
15. Gironès J, Lopez J, Vilaseca F, Herrera-Franco P, Mutje P. Biocomposites from *Musa textilis* and polypropylene: evaluation of flexural properties and impact strength. *Compos Sci Technol.* 2011;71(2):122–8. <https://doi.org/10.1016/j.compscitech.2010.10.012>.
16. Jiyas N, Sasidharan I, Bindu Kumar K, Gopakumar B, Dan M, Sabulal B. Mechanical superiority of Pseudoxynanthera bamboo for sustainable engineering solutions. *Sci Rep.* 2023;13(1):18169. <https://doi.org/10.1038/s41598-023-45523-3>.
17. Li X, Tabil LG, Panigrahi S. Chemical treatments of natural fiber for use in natural fiber-reinforced composites: a review. *J Polym Environ.* 2007;15:25–33. <https://doi.org/10.1007/s10924-006-0042-3>.
18. Goriparthi BK, Suman K, Rao NM. Effect of fiber surface treatments on mechanical and abrasive wear performance of polylactide/jute composites. *Compos A Appl Sci Manuf.* 2012;43(10):1800–8. <https://doi.org/10.1016/j.compositesa.2012.05.007>.
19. Chandrasekar M, Ishak M, Sapuan S, Leman Z, Jawaaid M. A review on the characterisation of natural fibres and their composites after alkali treatment and water absorption. *Plast Rubber Compos.* 2017;46(3):119–36. <https://doi.org/10.1080/14658011.2017.1298550>.
20. Yan L, Chouw N, Yuan X. Improving the mechanical properties of natural fibre fabric reinforced epoxy composites by alkali treatment. *J Reinf Plast Compos.* 2012;31(6):425–37. <https://doi.org/10.1177/0731684412439494>.
21. Sahu P, Gupta M. A review on the properties of natural fibres and its bio-composites: effect of alkali treatment. *Proc Inst Mech Eng L J Mater Des Appl.* 2020;234(1):198–217. <https://doi.org/10.1177/1464420719875163>.
22. Al-Mulla EAJ, Yunus WMZW, Ibrahim NAB, Rahman MZA. Properties of epoxidized palm oil plasticized poly(lactic) acid. *J Mater Sci.* 2010;45:1942–6. <https://doi.org/10.1007/s10853-009-4185-1>.
23. Zych A, Perotto G, Trojanowska D, Tedeschi G, Bertolacci L, Francini N, et al. Super tough polylactic acid plasticized with epoxidized soybean oil methyl ester for flexible food packaging. *ACS Appl Polym Mater.* 2021;3(10):5087–95. <https://doi.org/10.1021/acsapm.1c00832>.
24. Ali FB, Awale RJ, Fakhruddin H, Anuar H. Plasticizing poly(lactic acid) using epoxidized palm oil for environmental friendly packaging material. *Malays J Anal Sci.* 2016;20:1153–8. <https://doi.org/10.17576/MJAS-2016-2005-22>.
25. Parameswaranpillai J, Ranggappa SM, Siengchin S, Jose S. Bio-based epoxy polymers, blends, and composites: synthesis, properties, characterization, and applications. Hoboken: Wiley; 2021. <https://doi.org/10.1002/9783527823604>.
26. Sharma S, Singh AA, Majumdar A, Butola BS. Tailoring the mechanical and thermal properties of polylactic acid-based bionanocomposite films using halloysite nanotubes and polyethylene glycol by solvent casting process. *J Mater Sci.* 2019;54:8971–83. <https://doi.org/10.1007/s10853-019-03521-9>.
27. Valapa RB, Pugazhenthii G, Katiyar V. Effect of graphene content on the properties of poly(lactic acid) nanocomposites. *RSC Adv.* 2015;5(36):28410–23. <https://doi.org/10.1039/C4RA15669B>.
28. Chieng BW, Ibrahim NA, Wan Yunus WMZ, Hussein MZ, Silverajah VSG. Graphene nanoplatelets as novel reinforcement filler in poly(lactic acid)/epoxidized palm oil green nanocomposites: mechanical properties. *Int J Mol Sci.* 2012;13(9):10920. <https://doi.org/10.3390/ijms130910920>.
29. Sharma S, Majumdar A, Butola BS. Tailoring the biodegradability of polylactic acid (PLA) based films and ramie-PLA green composites by using selective additives. *Int J Biol Macromol.* 2021;181:1092–103. <https://doi.org/10.1016/j.ijbiomac.2021.04.108>.
30. Yan L, Chouw N, Yuan X. Improving the mechanical properties of natural fibre fabric reinforced epoxy composites by alkali treatment. *J Reinf Plast Compos.* 2012;31:425–37. <https://doi.org/10.1177/0731684412439494>.
31. Thampi AD, John AR, Arif MM, Rani S. Evaluation of the tribological properties and oxidative stability of epoxidized and ring opened products of pure rice bran oil. *Proc Inst Mech Eng J J Eng Tribol.* 2021;235(6):1093–100. <https://doi.org/10.1177/1350650120950535>.
32. Hasan M, Hoque ME, Mir SS, Saba N, Sapuan SM. Manufacturing of coir fibre-reinforced polymer composites by hot compression technique. In: Salit M, Jawaaid M, Yusoff, N, Hoque M (Eds) Manufacturing of natural fibre reinforced polymer composites. Springer, Cham. 2015. [https://doi.org/10.1007/978-3-319-07944-8\\_15](https://doi.org/10.1007/978-3-319-07944-8_15).
33. Baley C, Gominia M, Breard J, Bourmaud A, Davies P. Variability of mechanical properties of flax fibres for composite reinforcement: a review. *Ind Crops Prod.* 2020;145:111984. <https://doi.org/10.1016/j.indcrop.2019.111984>.
34. Porras A, Maranon A. Development and characterization of a laminate composite material from polylactic acid (PLA) and woven bamboo fabric. *Compos B Eng.* 2012;43(7):2782–8.
35. Jones RM. Mechanics of composite materials. 2nd ed. Boca Raton: CRC Press; 1999. <https://doi.org/10.1201/9781498711067>.
36. Munisamy, Sakthivel, Ramesh S. Mechanical properties of natural fibre (Banana, Coir, Sisal) polymer composites. *Science Park, (ISSN: 2321-8045).* 2013;1:1–6.
37. Alavudeen A, Thiruchitrabalam M, Narayanan V, Athijayamani A. Review of natural fiber reinforced woven composite. *Rev Adv Mater Sci.* 2011;27:146–50.

38. Bond I, Hucker M, Weaver P, Bleay S, Haq S. Mechanical behaviour of circular and triangular glass fibres and their composites. *Compos Sci Technol.* 2002;62(7):1051–61. [https://doi.org/10.1016/S0266-3538\(02\)00035-0](https://doi.org/10.1016/S0266-3538(02)00035-0).
39. Zhang Y, Li Y, Ma H, Yu T. Tensile and interfacial properties of unidirectional flax/glass fiber reinforced hybrid composites. *Compos Sci Technol.* 2013;88:172–7. <https://doi.org/10.1016/j.compscitech.2013.08.037>.
40. Nishino T, Hirao K, Kotera M, Nakamae K, Inagaki H. Kenaf reinforced biodegradable composite. *Compos Sci Technol.* 2003;63(9):1281–6. [https://doi.org/10.1016/S0266-3538\(03\)00099-X](https://doi.org/10.1016/S0266-3538(03)00099-X).
41. Shibata M, Ozawa K, Teramoto N, Yosomiya R, Takeishi H. Biocomposites made from short abaca fiber and biodegradable polyesters. *Macromol Mater Eng.* 2003;288(1):35–43. <https://doi.org/10.1002/mame.200290031>.
42. Nasir ANM, Romli A, Abdul Wahab MA. Properties of epoxidised palm oil (EPO)/styrene butadiene rubber (SBR) compound. *Adv Environ Biol.* 2014;8:2589–93.

**Publisher's Note** Springer Nature remains neutral with regard to jurisdictional claims in published maps and institutional affiliations.